# Accepted Manuscript

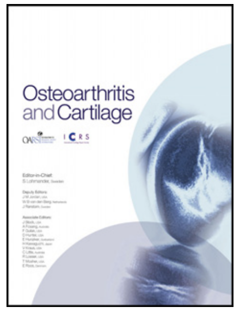


Non-destructive evaluation of articular cartilage defects using near-infrared (NIR) spectroscopy in osteoarthritic rat models and its direct relation to Mankin Score

Isaac Afara, Indira Prasadam, Ross Crawford, Yin Xiao, Adekunle Oloyede

PII: S1063-4584(12)00883-7

DOI: 10.1016/j.joca.2012.07.007

Reference: YJOCA 2695

To appear in: *Osteoarthritis and Cartilage*

Received Date: 12 January 2012

Revised Date: 29 June 2012

Accepted Date: 12 July 2012

# Non-destructive evaluation of articular cartilage defects using near-infrared (NIR) spectroscopy in osteoarthritic rat models and its direct relation to Mankin Score

Isaac Afara[1,2], Indira Prasadam[2], Ross Crawford[2, 3], Yin Xiao[1,2], Adekunle Oloyede[1,2]

[1] School of Chemistry, Physics and Mechanical Engineering, Science and Engineering Faculty, Queensland University of Technology, Brisbane, Australia.

[2] Institute of Health and Biomedical Innovation, Queensland University of Technology, Brisbane, Australia

[3] Prince Charles Hospital, Brisbane, Queensland, Australia.

**Running title:** Non-destructive assessment of cartilage defects with near-infrared spectroscopy

**Keywords:** Articular cartilage; near infrared (NIR) spectroscopy; osteoarthritis; non-destructive evaluation; Mankin score.

***Corresponding author***

Prof. Adekunle Oloyede PhD., DIC.

School of Engineering Systems, Faculty of Built Environment and Engineering

Queensland University of Technology

2 George St, GPO. Box 2434 Brisbane, Australia

Email: k.oloyede@qut.edu.au

Tel: +61 7 3138 2158

Fax: +61 7 3864 1516

## ABSTRACT

**Objective:** The aim of this study was to demonstrate the potential of near-infrared (NIR) spectroscopy for categorizing cartilage degeneration induced in animal models.

**Method:** Three models of osteoarthritic degeneration were induced in laboratory rats via one of the following methods: (i) menisectomy (MSX); (ii) anterior cruciate ligament transaction (ACLT); and (iii) intra-articular injection of mono-ido-acetete (1 mg) (MIA), in the right knee joint, with 12 rats per model group. After 8 weeks, the animals were sacrificed and tibial knee joints were collected. A custom-made near infrared (NIR) probe of diameter 5 mm was placed on the cartilage surface and spectral data were acquired from each specimen in the wavenumber range 4 000 – 12 500 $cm^{-1}$. Following spectral data acquisition, the specimens were fixed and Safranin–O staining was performed to assess disease severity based on the Mankin scoring system. Using multivariate statistical analysis based on principal component analysis and partial least squares regression, the spectral data were then related to the Mankin scores of the samples tested.

**Results:** Mild to severe degenerative cartilage changes were observed in the subject animals. The ACLT models showed mild cartilage degeneration, MSX models moderate, and MIA severe cartilage degenerative changes both morphologically and histologically. Our result demonstrate that NIR spectroscopic information is capable of separating the cartilage samples into different groups relative to the severity of degeneration, with NIR correlating significantly with their Mankin score ($R^2$ = 88.85%).

**Conclusion:** We conclude that NIR is a viable tool for evaluating articular cartilage health and physical properties such as change in thickness with degeneration.

## 1. INTRODUCTION

Articular cartilage is a highly specialized connective tissue covering the ends of articulating joints, and transmits high loads without developing unacceptably high stress [1]. This function can be compromised by wear, tear, and eventual erosion resulting from degenerative conditions like osteoarthritis (OA). With its onset often characterized by surface roughening and irregularity leading to focalized lesions, OA causes pain and inflammation in the affected joint. Sufficient grading of lesion severity at an early disease stage is critical for clinical decisions during treatment.

Arthroscopy and MRI are commonly used techniques for diagnosing joint abnormalities. Arthroscopy allows detailed description of the depth and extent of lesions [2, 3]; however, the detection of early stage, low-grade lesions is often unreliable because of the subjective nature of this technique, arguably the reason for the large discrepancies in assessments between clinicians. Alternatively, techniques such as MRI are used for evaluating chondral lesions, but traditional MRI does not have the resolution to detect initial lesions [4, 5]. Given the limited sensitivity of current options, there is a need for improved diagnostic methods for detecting the various degrees of OA lesions both precisely and in real-time during arthroscopic surgery.

At the histological level, OA is often categorized using the 14-point histological grading scale devised by Mankin *et al* [6]. Although this method has been effective for overall matrix grading, it requires destructive excision (biopsy) of part of the diseased tissue for histological evaluation, with this taking days or weeks to perform, and therefore not suitable for surgical applications where time and cost are critical parameters. Consequently, a number of intra-articular probes have been proposed and are being researched, with the aim of non-destructive and improved diagnostic accuracy of cartilage defect in real-time. These include ARTSCAN–an indentation-based device [7]; Infrared fiber optic probe (IFOP) [8]; and arthroscopic Optical Coherence Tomography (OCT) probe [9]. This study proposes the use of near infrared (NIR) spectroscopy.

NIR spectroscopy is a type of vibrational spectroscopy which produces spectral feedback when the NIR light is applied to a sample via a probe. A typical spectrum contains regions that represent CH, NH, OH and SH bonds, which are the fundamental building blocks of organic materials. These polymeric chains are also present to different degrees in cartilage, thereby underlying the potential applicability of NIR for cartilage evaluation. NIR penetrates deeper into the tissue than any other spectroscopic method including conventional infrared (IR) spectroscopy and is capable of generating results rapidly from intact cartilage matrices. The potential for non-destructive NIR probing of articular cartilage has been studied by a number of researchers [10-14]. We have recently correlated NIR spectra with cartilage viability [15].

The conditions and requirements for adapting NIR for assessing the integrity of articular cartilage have not been reported in the literature. Questions such as whether or not probe vibration during sample scanning affects the output spectrum, and the regions of the spectrum suitable for reliable evaluation of the tissue's structural viability, require answering. This study establishes and validates the correlation between sections of the NIR spectrum of articular cartilage and its Mankin score, especially as the absorption band of OH in materials with high water content, such as articular cartilage, is known to be easily saturated [16]. Besides establishing relationships, its validation is crucial for dependable practical use. These issues have not been reported in the research literature in this area. While taking these conditions and analytical requirements into account, this study primarily focuses on the potential of NIR for non-destructively determining the Mankin score for degraded cartilage to categorize degeneration and distinguish one between samples leading to potential application in real-time during surgery. Standard multivariate analytical approach based on principal component analysis (PCA) and partial least square (PLS) regression algorithm were utilized for correlating the NIR spectrum of the tissue to its Mankin score.

## 2. METHODOLOGY

**2.1 Animals:** Animal ethics approval for this project was granted from the QUT and Prince Charles Hospital Ethics Committees (Ethics number: 0900001134). Male Wistar Kyoto rats (11–12 weeks old) were purchased from the Medical Engineering Research Facility (Brisbane, Australia), each animal weighing approximately 320 g. The animals were housed under conditions that included a controlled light cycle (light/dark: 12 h each) and controlled temperature (23 ± 1°C), and were allowed to habituate themselves to the housing facilities for at least 7 days before surgeries.

**2.2 Rat OA models:** Three types of OA models were used in this study; two of which were surgically induced, and the third chemically induced. The surgical methods included (i) removing the medial compartment meniscus disk (MNX), or (ii) transecting anterior cruciate ligament (ACLT). The chemically induced method involved a single intra-articular injection of mono-ido-acetate (MIA). Briefly, for the MNX model, after giving anaesthesia Zoletil (tiletamine 15 mg/kg, zolazepam 15 mg/kg) and Xylazil (xylazine 10 mg/kg) the medial collateral ligament was transected just below its attachment to the meniscus, so that when the joint space opens, the meniscus was reflected toward the femur. The meniscus was cut at its narrowest point without damaging the tibial surface resulting complete medial meniscus transection. The surgical wound was closed by suturing in two layers. A sham group was subjected to the same surgical procedure on the left knee but without the excision of the ligament or meniscus manipulation. For the ACLT model, the right knee was exposed through a medial parapatellar approach. The patella was dislocated laterally and the knee placed in full flexion followed by ACL transection with micro-scissors. The joint capsule and subcutaneous layer were sutured separately and the skin was closed by vicryl 3.0. A sham group underwent the same surgical procedure with the omission of ACL transaction. After the surgery both the MNX and ACLT animals received pain killer (Buprenorphine 0.05 mg/kg) and antibiotic (Gentamycin (5 mg/kg). For the MIA model, the rats were anaesthetized and MIA injected (1 mg in 50 microliter volume in 0.9% saline) into the right joint cavity through the patellar ligament; control animals were injected with 0.9% saline only. A total of 36 rats were tested, with 12 rats in each group and no animal was excluded during the experiments.

### 2.3 Sample Preparation and NIR spectroscopy data acquisition

Eight weeks after surgery, the animals were euthanized and the whole knee joints removed by dissection and NIR readings were immediately taken as described below.

#### 2.3.1 Near Infrared spectroscopy - instrumentation and data acquisition

Diffuse reflectance NIR spectroscopy was performed using a Bruker MPA™ FT-NIR (Fourier Transform NIR) spectroscope (Bruker Optics, Germany), with detector spanning the full NIR spectral range. The spectroscope is equipped with a custom-made fibre optic probe of 5 mm outer diameter and 2 mm window diameter. It consists of a centrally placed 600 µm fibre for transmitting the NIR light, and six peripherally positioned 600 µm fibres for collecting the diffusely reflected light from the tissue. The spectroscope was connected to a

PC running OPUS 6.5 software (Bruker Optics, Germany) for equipment triggering and spectral data acquisition**.**

From preliminary experiments to investigate non-tissue factors that could affect the NIR signal, we observed that offset from the tissue's surface and vibration of the probe when hand-held for scanning significantly affected the repeatability of the output spectra. To minimize the effects of these factors, an experimental rig was constructed to keep the probe stable during scanning **(Fig 1a&b)**. The rig consists of a steel plate holding the specimen, placed in position on an adjustable x-y base plate. This plate sits directly under a z-axis guide which holds the probe in position. Prior to sample scanning, a reference spectrum was taken from a spectralon reflectance standard – *SRS-99* (Labsphere Inc., North Sutton, USA). The probe was gently lowered to touch the specimen's surface (without inducing deformation) and locked firmly in position. A mirror attached to the rig and perpendicular to the sample surface was used to determine contact between probe and sample surface. Spectral data was obtained over the full wavelength range at 16 $cm^{-1}$ resolution, with each spectrum consisting of 64 co-added scans; where this scanning condition was established as optimal and adequate for NIR probing of articular cartilage in our preliminary experiments. A single scan was taken from a relatively flat region on each joint. This is sufficient since each scan is the average of 64 individual scans. It was also ensured that any further analyses were conducted on tissue extracted from the same region as that exposed to NIR.

### 2.3.2 Morphological and histological characterization of OA samples

After the central portion of each joint was scanned, they were fixed in 4% paraformaldehyde and decalcified in 10% EDTA over a period of 2-3 weeks. Following decalcification, cartilage (surface-to-bone) matrix was carefully extracted for histological grading based on Mankin score from the region of the joint that was subjected to NIR probing. After dehydration and paraffin embedding, serial 5 μm sagittal sections were cut from the lateral and medial compartment of the joint. Two sections obtained at 100 μm intervals from the non weight-bearing and weight-bearing regions of each knee joint were stained with safranin O–fast green. For Safranin-O/Fast Green staining, 5 μm paraffin-embedded sections of tibia from mice were counterstained with Haematoxylin before being stained with 0.02% aqueous

Fast Green for 4 min (followed by 3 dips in 1% acetic acid) and then 0.1% Safranin-O for 6 min. The slides were then dehydrated and mounted with crystal mount medium. OA severity in the tibial plateau was evaluated according to modified Mankin's histologic grading system [6], and a cartilage destruction score was assigned for each knee sample by three independent assessors. The Mankin score assesses structure (0–6 points), cellularity (0–3 points), matrix staining (0–4 points), and tidemark integrity (0–1points), with a maximum score of 14 points. The final score for each sample was based on the most severe histological changes observed in multiple sections from each specimen. The Mankin's score was again divided into three stages depending on the score: grade I (normal cartilage, 0–1 points), grade II (mild to moderate degenerative change, 2–9 points), and grade III (severe degenerative change, ≥10 points. 12 rats were assessed in each group, giving a total of 36 rats for all tests.

The thickness of articular cartilage with progression of degeneration in the medial compartment tibial knee was measured semi automatically using ImageJ software (http://rsbweb.nih.gov/ij/). Measurements were obtained from sections stained with Safranin-O which provided excellent colour discrimination between bone and cartilage. The regions of interest on the femoral condyles were drawn using software and divided on the basis of the load-bearing areas of the knee during locomotion. The full thickness of each sample was determined by measuring the distance from the medial compartment of superficial border of non-calcified cartilage to the boundary with the calcified cartilage. For each condylar section, the average of three measurements was used. These measured thickness values were also correlated with the NIR spectra obtained from the corresponding knee.

### 2.3.3 Statistical evaluation and spectral analyses

Statistical analyses for the Mankin score and cartilage thickness were performed on Graphpad Prism (version 4.0). The data were expressed as mean ± 95% confidence interval (CI) and were compared using one-way ANOVA, a p-value of less than 0.05 was considered to be statistically significant.The normal distribution assumption was tested and passed for all groups prior to analysis. Because of the relatively small sample size (N = 36, 12 samples/group), power analysis (using G*Power statistical power analysis software [17]) was used to compute sample size effect, testing whether or not the quantity used is sufficient for

ANOVA. An effect size f = 0.946 was obtained which is adequate relative to the effect size convention proposed by Cohen [18].

Principal component analysis (PCA), a feature extraction method commonly used for NIR spectral analysis [19, 20], was employed to identify inherent patterns in the spectral data and also to reduce data dimensionality to a few uncorrelated variables (principal components – PC). Scores representing first and second PCs explaining variation in the original spectral data were obtained and used to characterize/group the samples. Spectral data were correlated with samples' Mankin scores using partial least squares (PLS) regression. This bilinear regression technique extracts factors from the predictor variables (NIR data), and regresses them to the response variable (Mankin score) [21]. The regression (calibration) models developed is then validated and used for predicting the response variables from predictors of unknown samples.

These techniques are best suited to modeling linear phenomena and therefore may not adequately model the raw data since some of the relationships between the spectra and cartilage properties may be non-linear or even multi-collinear. Hence, non-linearities such as those resulting from light scattering variations in reflectance spectroscopy [22] are often corrected/linearized using preprocessing algorithms including multiplicative scatter correction (MSC), straight line subtraction, standard normal variate (SNV), and derivative pretreatment. Of all these preprocessing techniques tested, it was observed that the relationship between the spectral data and the Mankin scores of the samples was optimized using a combination of first derivative and SNV techniques. First derivative pretreatment was used to correct for baseline variations since derivatized spectra are generally free of baseline because the derivative of any function eliminates constant variables [23]. SNV effectively removes the multiplicative interference of factors such as scatter, particle size and multi-collinearity [24].

To investigate the potential of NIR for predicting the tissue's structural integrity, specific regions (**Table 1**) of the whole spectrum were individually considered in the analyses. Each region was separately preprocessed and correlated to the Mankin score of the tissue using the single **y**-variable PLS (PLS1) algorithm. Leave-one-out (LOO) cross-validation method was used in the validation process to determine the optimal number of PLS factors, and to estimate the performance of the calibration models developed. This validation method was adopted because it is effective in analyzing small sample sizes. To avoid under- or overfitting, optimal model selection was based on the lowest root mean square error of cross-validation (RMSECV), and the highest $R^2$. All spectral analyses were performed using the OPUS Quant2 software suite (Bruker Optics, Germany).

## 3. RESULTS

Significant morphological differences were seen in the ACLT, MSX and MIA OA models compared to controls **(Fig. 2a)**, resulting in histological changes that resembled those occurring in stages of human OA. These differences are consistent with variations in the spectra (**Fig. 1b**) of the samples. Reduction of cartilage proteoglycan, extensive alterations characterized by marked hypercellularity due to cloning, numerous osteophytes on the margins, and decrease in the cartilage thickness were evident in the models compared to controls **(Fig. 2b)**. There were, however, significant differences relative to the speed of OA progression between the ACLT, MSX and MIA models. The severity of histological changes in the tissue was evaluated using a modified Mankin scale. The mean scores of the Mankin scale for the sham, ACLT, MSX, and MIA groups were $0.0 \pm 0.0$, $6.0 \pm 0.8$, $8.5 \pm 1.5$ and $12.4 \pm 2.2$ at week 8 respectively **(Fig. 2c)**. These results indicate that ACLT produces mild, MSX moderate, and MIA severe OA changes after 8 weeks. Consistent with the increase in Mankin score, decrease in the cartilage thickness in the models were observed relative to the controls **(Fig. 2d)**.

The effect of tissue degradation on the NIR spectra of each group can be observed from the PCA results, presented in **Fig. 3** as scores plot of the 1$^{st}$ and 2$^{nd}$ principal components (PC) of the NIR spectra for all samples tested. The samples group according to their level of degeneration along the 1$^{st}$ PC, while the samples within a group are distributed/classified along the 2$^{nd}$ PC. The samples can also be observed to group into two main classes along the 2$^{nd}$ PC axis: "class 1" consisting of the ACL samples with low Mankin score and arguably representative of early stage degeneration, and "class 2" encompassing the MSX and MIA treated models possessing relatively high Mankin score and characterized by relatively high to severe osteoarthritic damage.

The PLS1 calibration and validation plots for the model based on region B are presented in **Fig. 4**. The significantly high correlation between the optical response and the tissue's structural integrity (Mankin score) in this region demonstrates the potential of NIR to accurately evaluate the severity of cartilage degeneration. Furthermore, PLS1-based correlation between the NIR spectra and the samples' thickness values also reveal a strong linear relationship (**Fig. 5**).

## 4. DISCUSSION

We have established a relationship between NIR absorbance characteristics of artificially induced degenerated cartilage matrix and its relative Mankin score. Since the majority of absorption peaks observed in the NIR region arise mainly from OH, CH, NH and SH bonds, which characterize cartilage matrix and indicate micro- and macroscopic changes in its structure. In addition, because of the capacity of NIR to monitor key chemical, physical and morphological properties of materials [25], changes in the structure of cartilage matrix can arguably be determined from its NIR spectrum. Hence, embedded in the NIR spectra of articular cartilage are latent information on its physical, structural, and functional characteristics.

As earlier stated, the PCA results (**Fig. 3**) show that the samples cluster according to their level of degeneration along the 1$^{st}$ PC axis. A reasonable and expected observation would be a case where the MSX group lie between the ACL and MIA groups along the 1$^{st}$ PC axis since its average Mankin score lies between those of the other two groups. This suggests that the relationship between the spectral PCs and the Mankin scores may not be linear as properties such as osteophytes and cell cloning may not directly influence its NIR spectral response. Also, because the Mankin score is a combination of several parameters, it is likely that the PCs are related to some parameters and not to others. The grouping of the samples into two main classes, representative of mild and severe osteoarthritic degeneration, along the 2$^{nd}$ PC axis (**Fig. 3**) provides an insight into the relationship between the tissue's absorption spectra and its Mankin score via the PC scores of the spectra. This can arguably be extended to explain the correlation between the NIR spectra and the individual components of the Mankin score of cartilage. However, this is beyond the scope of the current study.

From **Table 1**, the models developed using regions A, B and D of the NIR spectra present significantly high correlations with Mankin score. In contrast, region C which covers the section of the spectra characterized by the water peak, demonstrates a weaker relationship with the Mankin score. This weak correlation would be expected to negatively influence the robustness and accuracy of any model developed using the whole spectrum for analysis. Hence, analysis based on specific regions of the spectrum present a more efficient option for correlation. Validation of the suitability of the regions chosen for the analysis (**Table 1**, column 3) beyond the calibration $R^2$ values (column 2) demonstrate that the choices are adequate for the prediction of the Mankin score intended.

If the model's predictive capacity were to be based on region C, the Mankin score of new samples would, undoubtedly, be very poor, with large prediction errors. However, regions A, B, and D demonstrated far better performance in predicting the score of new samples with low prediction error. Region A presents the best potential for clinical application (column 3 of **Table 1**). The poor performance of region C can be attributed to the masking effect of the water peak resulting from severe absorption of NIR light by the OH bond in water molecules. This poor performance and relatively high prediction error confirms that region C is of little use in correlation analyses of cartilage NIR spectra for the purpose of assessment. It is emphasized that the exclusion of this region does not affect the correlation results of the other regions.

While region A presents the best validation result, absorptions in this region are characterized by third overtone bond vibrations which tend to be weak. Hence, care should be exercised when using this region for predictive purposes in cartilage evaluation. Region B encompasses regions characterized by second overtone $CH_n$ vibrations and is arguably representative of the major matrix components; collagen and proteoglycans. The vibrations likely to be characteristic of region D include first overtone $CH_n$ and SH stretch vibrations, which is arguably due to the proteoglycan content of articular cartilage.

This research presented in this paper is significant in contributing to the knowledge that could advance the non-destructive evaluation of cartilage integrity in real-time with potential benefit to surgery. The region-specific analysis developed presents a computationally faster option to using the whole spectrum since the amount of spectral data involved in the analysis is reduced. This means that less time is required for analyses, which includes model development, and application (prediction).

Idealizing the thickness of articular cartilage as the effective pathlength of the NIR light as it traverses from the surface of the tissue, through the translucent matrix, down to the optically opaque subchondral bone is a plausible reason for this high correlation. Essentially, a thick sample would present more matrix material and more spectral absorption than a thinner sample. This high correlation (**Fig. 5**) also demonstrates the capacity of NIR for accurately tracking physical/morphological changes in the matrix, via thickness in this case, with disease progression. This result is supported by the study of Faris *et al* [26] where the penetration depth of NIR in human neonatal head was shown to be up to 8.5 mm. While this is a promising result with potential clinical relevance in arthroscopic procedures, the limitations associated with the method, such as probe vibration during hand-held scanning, would require engineering aid for stabilization (e.g. systems similar to the autofocus devices in cameras) before it may be considered for cartilage evaluation in real-time during surgery. The region where the correlation is optimized (6102 – 5446 $cm^{-1}$), is characteristic of the 1$^{st}$ overtone $CH_n$ and SH absorptions, that arguably indicate collagens and proteoglycans.

The analytical approach adopted in the current study, based on multivariate analysis, presents a more accurate and robust means of adapting NIR for cartilage evaluation. This is unlike the method employed by Spahn *et al.* [10, 11] and Hoffman *et al.* [12], who proposed the evaluation of cartilage defects using NIR spectroscopy via a parameter (AR) calculated as the ratio of peak absorptions of two major bands (the first OH and CH overtones, and the second CH overtone). AR was argued to be an indicator of the water content within cartilage. However, in conventional NIR spectroscopic analysis of materials with high water content, like articular cartilage, the absorption bands due to OH bonds in water (1400 to 1500 nm) tend to be overwhelming [16], causing severe absorption of the NIR light (saturation). This yields spectral data with very little discernible information and poor analytical relevance. This is arguably the reason for the lack of discrimination between grade 1 and 2 cartilage lesions [7] using AR. We have shown in the current study that this region is inefficient for assessing articular cartilage (**Table. 1**). Utilizing multivariate analysis, coupled with spectral preprocessing and wavelength selection based on distinct regions, the correlation between the spectra and the properties of the tissue is optimized as exhibited by the clear distinction between the different osteoarthritic models tested (**Fig. 3**), and accurate estimation of their Mankin score and thickness (**Fig. 4 & 5**).

**Conclusion:** We have evaluated the potential of NIR spectroscopy for quantifying tissue alterations in OA animal models. Mankin grade, histology, and loss of tissue matrix, measured via the cartilage thickness, were found to correlate significantly with the NIR absorption spectra, leading to potential NIR quantitative evaluation of cartilage defects.

Finally, this method has the potential to facilitate real-time non-destructive evaluation of cartilage defects arthroscopically.


## ACKNOWLEDGEMENT

We thank the National Health and Medical Research Council (NHMRC) Australia, and Queensland University of Technology, Brisbane, Australia for partly funding this project. This research was also partially supported by the Prince Charles Hospital Foundation (MS2010-02).


## AUTHOR CONTRIBUTION

Contributions by the authors to the preparation of this manuscript are as follows:

**Isaac Afara:** Experimental design, conduction of laboratory experiment, multivariate correlation and statistical analysis, and preparation of the manuscript.

**Indira Prasadam:** Experimental design, conduction of laboratory experiment, histological evaluation and analysis, and preparation of the manuscript.

**Ross Crawford:** Clinical input and guidance, editing manuscript.

**Yin Xiao:** Guidance in experimental design and analysis, editing manuscript.

**Adekunle Oloyede:** Guidance in experimental design and data analysis, writing and editing manuscript.

## CONFLICT OF INTEREST

We hereby declare that there is no conflict of interest, whether personally or professionally, regarding this paper titled “*Non-destructive evaluation of articular cartilage defects using near-infrared (NIR) spectroscopy in osteoarthritic rat models and its direct relation to Mankin Score*” which has been submitted for publication in Osteoarthritis and Cartilage.

## REFERENCES


[1] Hunziker, E.B., Articular cartilage repair: basic science and clinical progress. A review of the current status and prospects. Osteoarthritis Cartilage, 2002. **10**(6): p. 432-63.

[2] Menche, D.S., Observer reliability in the arthroscopic classification of osteoarthritis of the knee. J Bone Joint Surg Br, 2003. **85**(3): p. 463-4; author reply 464.

[3] Brismar, B.H., Wredmark, T., Movin, T., Leandersson, J., and Svensson, O., Observer reliability in the arthroscopic classification of osteoarthritis of the knee. J Bone Joint Surg Br, 2002. **84**(1): p. 42-7.

[4] Sanders, T.G., Imaging of the postoperative knee. Semin Musculoskelet Radiol, 2011. **15**(4): p. 383-407.

[5] Gopez, A.G. and Kavanagh, E.C., MR imaging of the postoperative meniscus: repair, resection, and replacement. Semin Musculoskelet Radiol, 2006. **10**(3): p. 229-40.

[6] Mankin, H.J., Dorfman, H., Lippiello, L., and Zarins, A., Biochemical and metabolic abnormalities in articular cartilage from osteo-arthritic human hips. II. Correlation of morphology with biochemical and metabolic data. J Bone Joint Surg Am, 1971. **53**(3): p. 523-37.

[7] Laasanen, M.S., Toyras, J., Hirvonen, J., Saarakkala, S., Korhonen, R.K., Nieminen, M.T., Kiviranta, I., and Jurvelin, J.S., Novel Mechano-acoustic Technique and Instrument for Diagnosis of Cartilage Degeneration. Physiological Measurement, 2002. **23**: p. 491 - 503.

[8] West, P.A., Bostrom, M.P.G., Torzilli, P.A., and Camacho, N.P., Fourier Transform Infrared Spectral Analysis of Degenerative Cartilage: An Infrared Fiber Optic Probe and Imaging Study. Applied Spectroscopy, 2004. **58**(4): p. 376-381.

[9] Pan, Y., Li, Z., Xie, T., and Chu, C.R., Hand-held arthroscopic optical coherence tomography for in vivo high-resolution imaging of articular cartilage. Journal of biomedical optics, 2003. **8**(4): p. 648-654.

[10] Spahn, G., Plettenberg, H., Kahl, E., Klinger, H.M., Muckley, T., and Hofman, G.O., Near-infrared (NIR) spectroscopy. A new method for arthroscopic evaluation of low grade degenerated cartilage lesions. Results of a pilot study. BMC Musculoskeletal Disord., 2007. **8**: p. 47.

[11] Spahn, G., Plettenberg, H., Nagel, H., Karl, E., Klinger, H.M., Muckley, T., Gunther, M., Hofman, G.O., and Mollenhauer, J.A., Evaluation of cartilage defect with near infrared spectroscopy (NIR): An ex vivo study. Medical Engineering and Physics, 2008. **30**: p. 285 - 292.

[12] Hofman, G.O., Marticke, J., Grossstuck, R., Hoffman, M., Lange, M., Plettenberg, H.K., Braunschweig, R., Schilling, O., Kaden, I., and Spahn, G., Detection and evaluation of initial cartilage pathology in man: A comparison between MRT, arthroscopy and near-infrared spectroscopy (NIR) in their relation to initial knee pain. Pathophysiology, 2010. **17**(1): p. 1-8.

[13] Brown, C.P., Bowden, J.C., Rintoul, L., Meder, R., Oloyede, A., and Crawford, R., Diffuse reflectance near infrared spectroscopy can distinguish normal from enzymatically digested cartilage. Phys. Med. Biol., 2009. **54**: p. 5579-5594.

[14] Baykal, D., Irrechukwu, O., Lin, P.-C., Fritton, K., Spencer, R.G., and Pleshko, N., Nondestructive Assessment of Engineered Cartilage Constructs Using Near-Infrared Spectroscopy. Applied Spectroscopy, 2010. **64**(10): p. 1160-1166.

[15] Afara, I., Sahama, T., and Oloyede, A. Near infrared for non-destructive testing of articular cartilage. In Nondestructive testing of materials and structures, Istanbul, Turkey. Springer, 2011: p. 367-372.

[16] Kradjel, C., NIR Analysis of Polymers. *In* 'Handbook of Near Infrared Analysis', A.D. Burns and E.W. Ciurczak, Editors, edition. Marcel Dekker, Inc., New York, 2001.

[17] Faul, F., Erdfelder, E., Lang, A.-G., and Buchner, A., G*Power 3: A flexible statistical power analysis program for the social, behavioral, and biomedical sciences Behavior Research Methods, 2007. **36**: p. 175-191.

[18] Cohen, J., Statistical Power Analysis for the Behavioural Sciences. 2nd ed. 1988, Hillsdale, New Jersey: Lawrence Erlbaum Associates, p.355.

[19] Devaux, M.F., Bertrand, D., Robert, P., and Qannari, M., Application of Principal Component Analysis on NIR Spectral Collection after Elimination of Interference by a Least-Squares Procedure. Appl. Spectrosc., 1988. **42**(6): p. 1020-1023.

[20] Togersen, G., Arnesen, J.F., Nilsen, B.N., and Hildrum, K.I., On-line prediction of chemical composition of semi-frozen ground beef by non-invasive NIR spectroscopy. Meat Science, 2003. **63**(4): p. 515-523.

[21] Bjørsvik, H.-R. and Martens, H., Data analysis: Calibration of NIR instruments by PLS regression. *In* 'Handbook of Near Infrared Analysis', A.D. Burns and E.W. Ciurczak, Editors, 2nd edition. Marcell Dekker, Inc., New York, 2001, p. 185-207.

[22] Geladi, P., MacDougall, D., and Martens, H., Linearization and scatter-correction for near infrared reflectance spectra of meat. Applied spectroscopy, 1985. **39**(3): p. 491-500.

[23] Brown, C.D., Vega-montoto, L., and Wentzell, P.D., Derivative preprocessing and optimal corrections for baseline drift in multivariate calibration. Applied Spectroscopy, 2000. **54**(7): p. 1055-1068.

[24] Barnes, R.J., Dhanoa, M.S., and Lister, S.J., Standard Normal Variate Transformation and Detrending for Near-Infrared Diffuse Reflectance Spectra. Applied Spectroscopy, 1989. **43**(5): p. 772-777.

[25] Ghosh, S. and Rodgers, J., NIR Analysis of Textiles. *In* 'Handbook of Near Infrared Analysis', A.D. Burns and E.W. Ciurczak, Editors, edition. Marcel Dekker, Inc., New York, 2001.

[26] Faris, F., Thorniley, M., Wickramasinghe, Y., Houston, R., Rolfe, P., Livera, N., and Spencer, A., Noninvasive Invivo near-Infrared Optical Measurement of the Penetration Depth in the Neonatal Head. Clinical Physics and Physiological Measurement, 1991. **12**(4): p. 353-358.

## FIGURE LEGENDS

**Figure 1:** (a) Experimental setup for near infrared spectral data acquisition, (b) Typical spectra of osteoarthritic models tested.

**Figure 2:** Characterization of OA changes in the animal models. **(a)** Representative macroscopic appearances of the tibial condyles at 8 weeks in sham and in three different OA models, where L stands for lateral compartment, and M for medial compartment. **(b)** Representative histology sections of tibial condyles at 8 weeks in sham and in three different OA models. Distal tibia was sectioned coronally and stained with safranin-O. The most degenerated area (medial part) of each sample is included. Scale bar = 200 ìm. ACLT= anterior cruciate ligament transaction induced OA model, MNX= menisectomy induced OA model and MIA=mono-ido-acetate chemical induced OA model **(c)** Quantitation of safranin-O stained sections using the Mankin histopathology scoring system. Values are the geometric mean ± 95% confidence interval (CI), $*p = 0.0041$ is considered significant. **(d)** Cartilage thickness measurements in sham and in three different animal models at week-8 were performed as described in the methodology. Values are the geometric mean ± 95% confidence interval (CI), $*p < 0.001$ (10 knees).

**Figure 3**: Score plot of the 1$^{st}$ and 2$^{nd}$ principal components of (first derivative + SNV) preprocessed NIR spectral data showing classification of the osteoarthritic cartilage models into distinct groups (n=36).

**Figure 4**: Relationship between NIR spectra and the structural integrity of the osteoarthritic cartilage models tested based on the Mankin score, (a) Calibration, and (b) Validation.

**Figure 5**: Correlation between NIR spectral data and the thickness of non-calcified cartilage from the osteoarthritic models, (a) Calibration, and (b) Validation. Thickness values from the tibia plateau were used here.

## TABLES

**Table 1:** PLSR assessment statistics of articular cartilage Mankin score to NIR correlation based on distinct regions of the spectrum, RMSEP = root mean square error of prediction [‡ indicates the region comprising the water peak of articular cartilage].

| | Region | Calibration $R^2$ (%) | Validation $R^2$ [R] (%) | RMSEP |
|---|---|---|---|---|
| A → | 12 436 - 9 967 $cm^{-1}$ | 95.28 | 88.85 [94.26] | 0.854 |
| B → | 10 500 - 7 500 $cm^{-1}$ | 94.33 | 86.82 [93.18] | 0.928 |
| C → | ‡7 213 - 6 434 $cm^{-1}$ | 63.18 | 35.59 [59.66] | 2.05 |
| D → | 6 113 - 5 446 $cm^{-1}$ | 98.44 | 85.01 [92.20] | 0.99 |

| | Region | Calibration $R^2$ (%) | Validation $R^2$ [R] (%) | RMSEP |
|---|---|---|---|---|
| A $\rightarrow$ | 12 436 - 9 967 $cm^{-1}$ | 95.28 | 88.85 [94.26] | 0.854 |
| B $\rightarrow$ | 10 500 - 7 500 $cm^{-1}$ | 94.33 | 86.82 [93.18] | 0.928 |
| C $\rightarrow$ | ‡7 213 - 6 434 $cm^{-1}$ | 63.18 | 35.59 [59.66] | 2.05 |
| D $\rightarrow$ | 6 113 - 5 446 $cm^{-1}$ | 98.44 | 85.01 [92.20] | 0.99 |

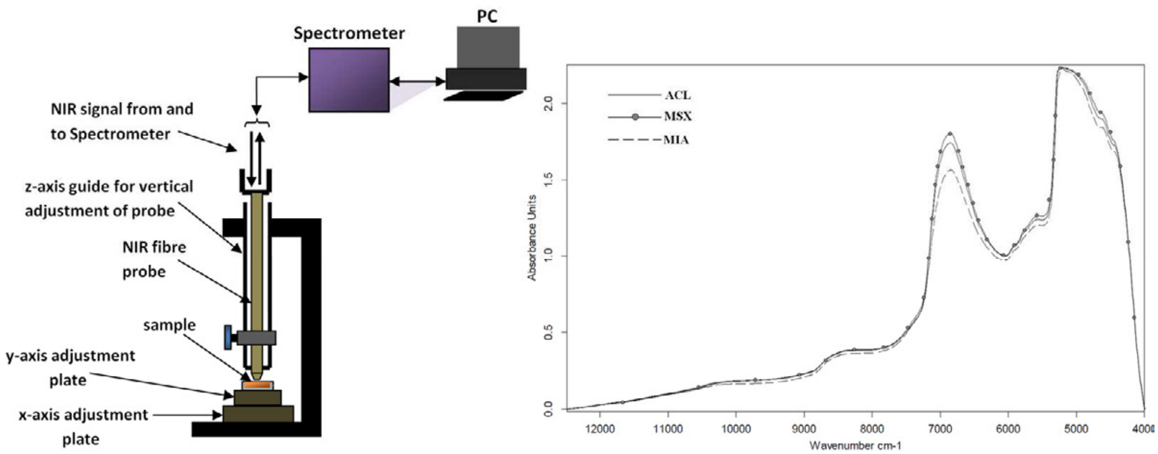
PC
Spectrometer
NIR signal from and
to Spectrometer
z-axis guide for vertical
adjustment of probe
NIR fibre
probe
sample
y-axis adjustment
plate
x-axis adjustment
plate
ACL
MSX
MIA
Absorbance Units
Wavenumber cm-1

(a) (b)

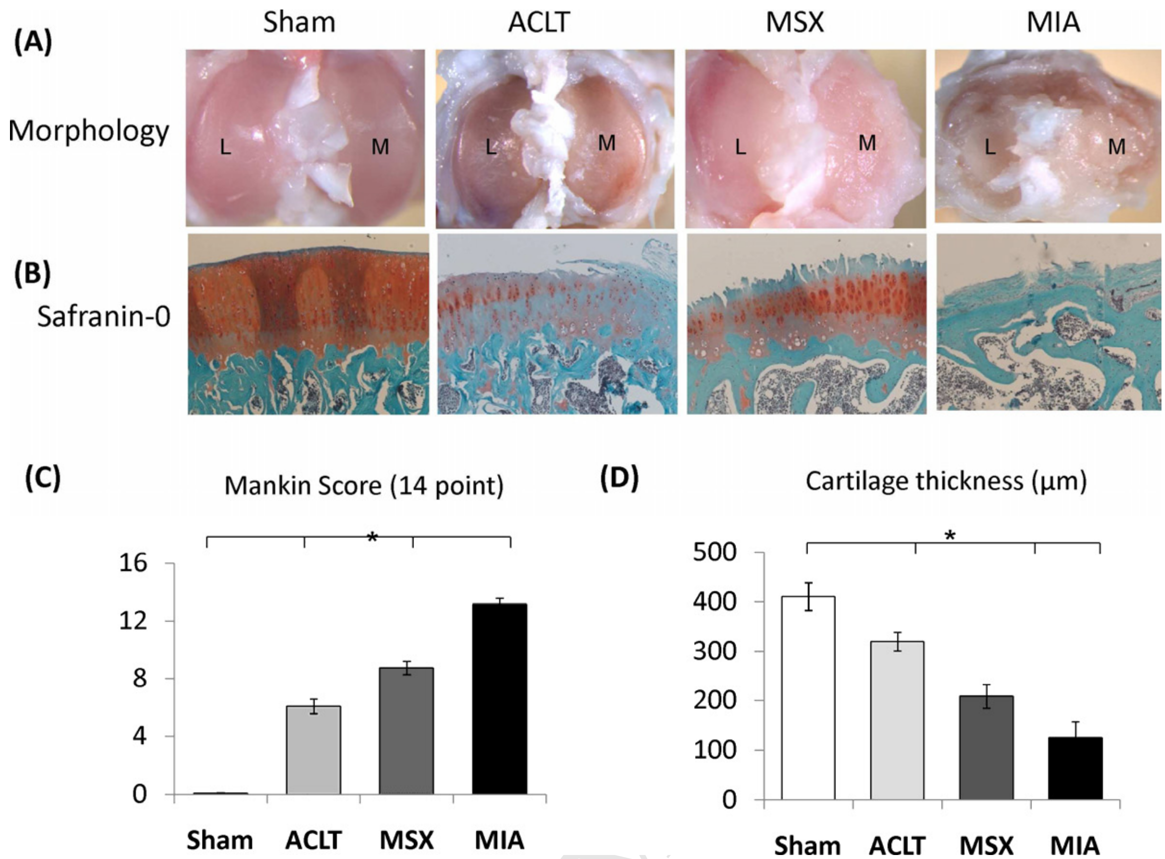
(A)
Sham
ACLT
MSX
MIA
Morphology
L
M
(B)
Safranin-0
(C)
Mankin Score (14 point)
*
16
12
8
4
0
Sham
ACLT
MSX
MIA
(D)
Cartilage thickness (μm)
*
500
400
300
200
100
0
Sham
ACLT
MSX
MIA

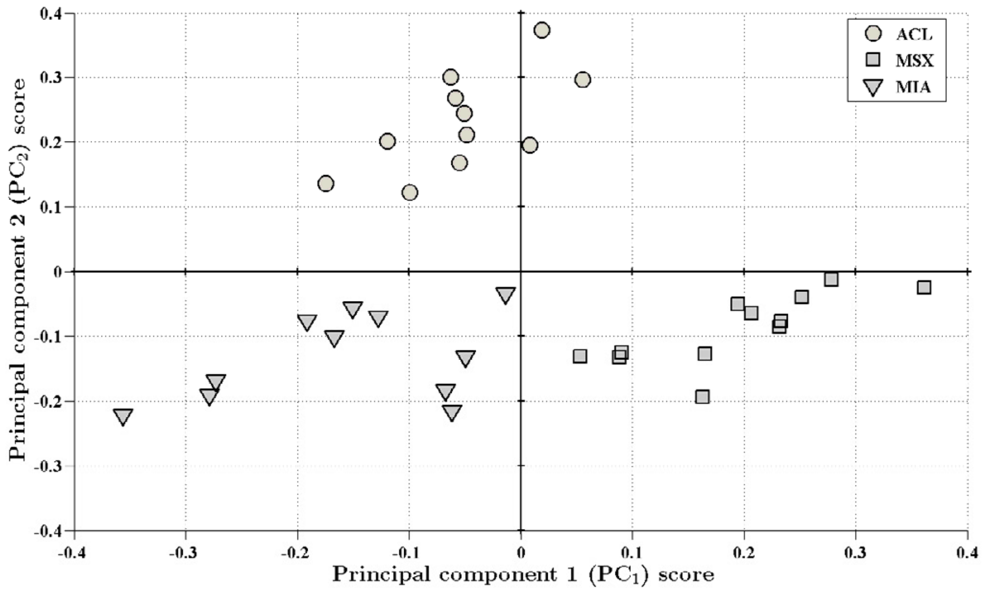

ACL
MSX
MIA
Principal component 2 ($PC_2$) score
Principal component 1 ($PC_1$) score
0.4
0.3
0.2
0.1
0
-0.1
-0.2
-0.3
-0.4

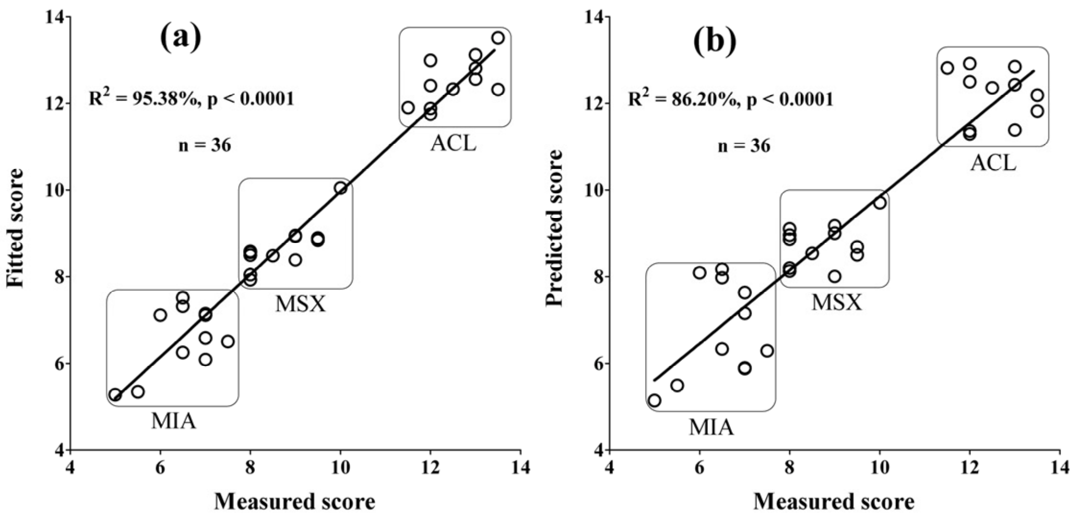
(a)
R$^2$ = 95.38%, p < 0.0001
n = 36
ACL
MSX
MIA
Fitted score
Measured score
(b)
R$^2$ = 86.20%, p < 0.0001
n = 36
ACL
MSX
MIA
Predicted score
Measured score

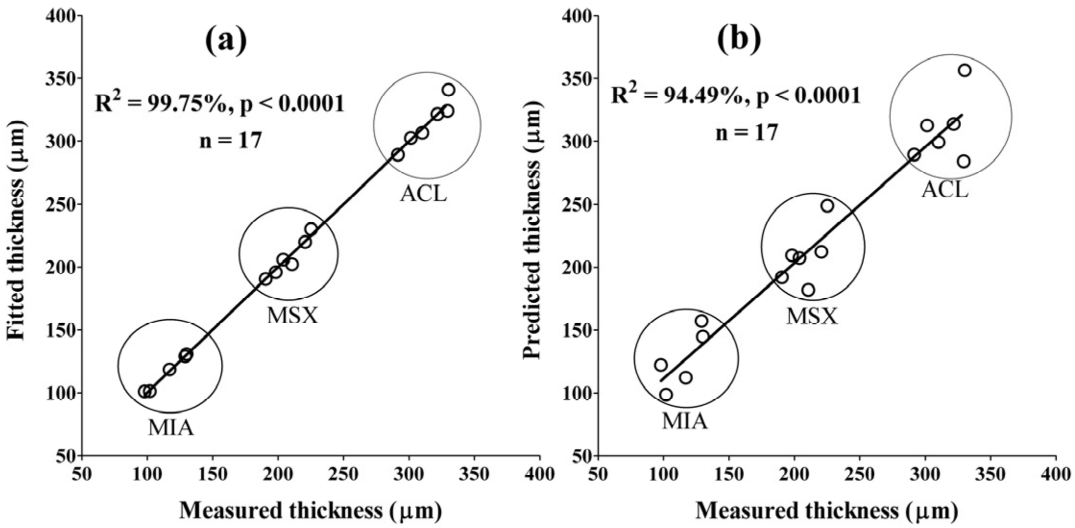

(a)
R² = 99.75%, p < 0.0001
n = 17
Fitted thickness (μm)
Measured thickness (μm)
ACL
MSX
MIA
(b)
R² = 94.49%, p < 0.0001
n = 17
Predicted thickness (μm)
Measured thickness (μm)
ACL
MSX
MIA